Chapter 3

To assess the efficacy of melatonin, GABA and combination therapy in amelioration of diabetic manifestations in high fat diet (HFD) induced T2D mouse model

3.1 Introduction

Lifestyle changes, including a tendency of nocturnality and consuming high-calorie foods, disrupt the natural sleep/wake cycle and circadian rhythms, favoring obesity, type 2 diabetes (T2D), and metabolic disorders in humans (Scheer et al., 2009). The pathogenesis of T2D is more complex, and involves different degrees of β-cell failure and insulin resistance. Inflammation, oxidative stress, metabolic and mitochondrial dysfunction, Insulin resistance in peripheral tissues, hyperleptinemia, hyperinsulinemia, and impede glucose regulation are hallmarks of T2D. Insufficient insulin action results in hyperglycemia and dyslipidemia, leading to gluco-lipotoxicity in multiple cell types, including pancreatic β-cells, further contributes to a decrease in β-cell mass and function (Lin and Sun, 2010). Despite the advances in DM management, the incidence and prevalence of this disease are increasing alarmingly. Thus, developing a novel biomolecule that can effectively aid diabetic manifestations in different organs besides increasing β-cell mass is pertinent.

Melatonin is functionally linked to glucose metabolism (Mulder et al., 2009) and is known to reduce obesity and T2D (Stumpf et al., 2009; Peshchke, 2008; Pan et al., 2006) by regulating glucose and lipid metabolism (Peschke and Muhlbauer, 2010; Rios-Lugo et al., 2010; Nduhirabandi et al., 2011) in both humans and rodents. The inverse relationship between insulin secretion and plasma melatonin concentration suggests a link between melatonin and T2D (Peschke et al., 2013). Further, the levels of melatonin decrease in both Goto Kakizaki rats and T2D patients with hyperinsulinemia (Peschke et al., 2006). Pinealectomy leads to melatonin loss, reduced glucose transporter type 4 (GLUT4) levels, glucose intolerance, and insulin resistance, as melatonin checks insulin secretion (Nishida et al., 2003; Lima et al., 1998). Chronic administration of melatonin has been demonstrated to decrease insulin resistance and enhance lipid metabolism in T2D rats (Nishida et al., 2002). Additionally, rodent studies have indicated that melatonin administration reduces HbA1c levels and body fat, and increases insulin sensitivity and GLUT4 expression in peripheral tissues in a diet-induced obese T2D mouse model (Karamitri & Jockers, 2019).

GABA has also previously demonstrated its efficacy in preventing T2D progression by improving glucose tolerance and insulin sensitivity in high-fat diet (HFD)-induced obese mice (Tian et al., 2011b; Rathwa et al., 2022). GABA improves hyperglycemia in STZ-induced

diabetic rats and high-fat diet (HFD)-induced diabetes by reducing gluconeogenesis and insulin resistance and increasing *GLUT4* mRNA expression (Rezazadeh et al., 2021; Sohrabipour et al., 2018; Rathwa et al., 2022). Tian et al. (2011b) have shown that oral GABA therapy can significantly decrease blood glucose levels and enhance glucose tolerance and insulin sensitivity in HFD-fed mice. Furthermore, they showed that the peripheral GABA receptor activation could prevent the HFD-induced insulin resistance. GABA-treated diabetic mice display greater plasma insulin levels, reduced glucagon levels, normalized glycemic control, and improved metabolic state (Liu et al., 2017). Ironically, a significant reduction in circulating GABA concentration was reported in T2D patients (Mohamed et al., 2015). These studies suggest a crucial role of GABA in ameliorating metabolic profile by improving the insulin signaling pathway, increasing the expression of *GLUT4* mRNA, and improving hyperglycemia and insulin resistance.

Our recent studies also suggest that melatonin (Patel et al., 2023) and GABA (Rathwa et al., 2022) separately can ameliorate T2D manifestations in HFD-induced T2D mouse model. Thus, we aimed to investigate the therapeutic potential of melatonin combined with GABA on diabetic manifestations in the HFD-induced T2D mouse models.

3.2 Materials and methods

3.2.1 Animals:

Forty young (6-7 weeks old) C57BL/6J male mice procured from ACTREC, Mumbai, were used for the experiment. The animals were maintained on a 12hr light-dark cycle starting at 7.00 AM. These animals had free access to standard chow/HFD diet (Keval Sales Corporation, Vadodara, India) and water. All the experimental procedures were conducted as per the Purpose of Control and Supervision of Experiments on Animals (CPCSEA) guidelines and were approved by Institutional Animal Ethical Committee (IAEC) (MSU/BC/09/2019).

3.2.2 Induction of T2D and treatment:

For T2D induction, 32 C57BL/6J mice were fed a HFD, and eight control mice were fed a normal chow diet (NCD) for 30 weeks. T2D was confirmed 30 weeks later in mice having FBG >200 mg/dL. HFD-fed mice were randomly assigned into four groups: i. HFD, ii. Melatonin (M) treated, iii. GABA (G) treated, and iv. M+G treated. Melatonin (Sigma, St.

Louis, MO, USA) was administered between 6 PM to 7 PM daily at 10 mg/kg BW i.p., dissolved in 0.1% ethanol and 0.9% saline (Patel et al., 2023). GABA (Sigma-Aldrich, United States), was given at a dose of 10 mg/day (Liu et al., 2017) by oral gavage. The HFD group received 0.1% ethanol in 0.9% saline and water as vehicle. The treatment was given for six weeks. FBG levels and BW were measured weekly, along with food and water intake.

3.2.3 Glucose tolerance and insulin tolerance tests:

The intraperitoneal glucose tolerance and intraperitoneal insulin sensitivity were evaluated by IPGTT and IPITT, respectively, at the end of treatment. For IPGTT and IPITT, all mice fasted for 6 hours and injected with glucose (2 g/kg BW i.p.) and insulin (0.75 U/kg BW), respectively. Blood glucose levels were measured immediately at 0, 15, 30, 60, 90, and 120 minutes by tail snipping method, using a Glucometer. The total area under the curve (AUC) was evaluated.

3.2.4 Metabolic and biochemical parameters:

Before sacrificing mice, 1 ml blood was collected into K_3EDTA tubes by the orbital sinus method for biochemical assays after 6 hours of fasting. Additionally, insulin sensitive tissues were harvested, which are further described in depth below. Blood was centrifuged at 6000 g for 5 minutes, and plasma was separated and stored at -20°C for further analysis. Plasma insulin, leptin, and melatonin were measured by commercially available mouse insulin, mouse leptin (both from RayBiotech, GA, USA), and mouse melatonin (Elabscience, Houston, TX, USA) ELISA kits as per the manufacturer's protocols. Lipid profile (triglycerides, total cholesterol, HDL-c) was measured by commercially available kits (Reckon Diagnostics Pvt. Ltd., Vadodara, GJ, India). Friedewald's (1972) formula was used for calculating Low-Density Lipoprotein (LDL).

3.2.5 Gene expression analyses:

Parts of the liver, skeletal muscle, and adipose tissue were stored in RNAlater™ Stabilization Solution (Thermo Fisher Scientific, USA) for gene expression analysis of the key glucoregulatory enzymes and *glucose transporter 2* (*GLUT2*), mitochondrial biogenesis, and lipid metabolism, respectively. Total RNA was extracted by Trizol method. RNA integrity and purity were checked by 1.5% agarose gel electrophoresis/ethidium bromide staining and a

260/280 absorbance ratio of 1.9, respectively. RNA was treated with DNase I (Puregene, Genetix Biotech) to avoid DNA contamination before cDNA synthesis. Transcriptor High Fidelity cDNA Synthesis Kit (Roche Diagnostic GmbH, Mannheim, Germany) was used to prepare cDNA using one microgram of total RNA isolated, according to the manufacturer's instructions in the Eppendorf Mastercycler gradient (USA Scientific, Inc., Florida, USA). The expression of targeted genes and glyceraldehyde 3-phosphate dehydrogenase (*GAPDH*) transcripts were monitored by LightCycler®480 Real-time PCR (Roche Diagnostics GmbH, Germany) using gene-specific primers (Eurofins, India), as shown in Table 3.1. The expression of *GAPDH* gene was used as a reference. Real-time PCR was performed as described previously by determining $2^{-\Delta\Delta Ct}$ (Patel et al., 2019).

3.2.6 Droplet digital PCR (ddPCR):

Gene expression of *MTNR1B* and *glucose transporter 4* (*GLUT4*) in mouse adipose tissue was monitored by ddPCR using EvaGreen dye (Bio-Rad, Hercules, CA, USA). Each ddPCR reaction contained 20 µl of the master mix, including 10 µl of Eva Green supermix, 0.5 µl (2.5 mM) forward and reverse primer each, 1 µl cDNA (50 ng), and 8 µl nuclease-free water. This system was loaded in a droplet generator cartridge with 70 µl of droplet generation oil into an oil well. QX200 TM Droplet Generator (Bio-Rad, Hercules, CA, USA) was used to generate droplets, which were loaded to 96 well PCR plate. The plate was heat-sealed with a foil and was run in a thermal cycler. The PCR conditions for the assay were: 95 °C for 5 min; 40 cycles of 95 °C for 30s and 60 °C (depending on annealing temperature) for 1 min; and three final steps at 4 °C for 5 min, 90 °C for 5 min, and a 4 °C for 30 min to boost dye stabilization. The PCR product was read in QX200TM Droplet Reader (Bio-Rad, Hercules, CA, USA) and was analyzed by QuantaSoft™ software (Bio-Rad, Hercules, CA, USA). The results were plotted as Ch1Amplitute and number of copies/µl. Blue droplets show a number of positive droplets for their respective target genes, and grey droplets indicate negative droplets for the target genes. Non-template control was run for each assay. The details of the forward and reverse primers are shown in Table 3.1.

Table 3.1. List of primers used for the transcript analysis.

Gene	Primer Sequence (5'-3')	Annealing Temperature	Amplicon Size	Tissue

Glucokinase (*GCK*)	**FP:** AGGAGGCCAGTGTAAAGATGT **RP:** TCCCAGGTCTAAGGAGAGAAA	56°C	90bp	Liver
Phosphoenol-pyruvate carboxykinase (*PEPCK*)	**FP:** CTGCATAACGGTCTGGACTTC **RP:** CAGCAACTGCCCGTACTCC	65°C	151bp	
Fructose bis-phosphatase 1 (FBP1)	**FP:** GCATCGCACAGCTCTATGGT **RP:** CTCAGGTTCGATTATGATGGC	59°C	170 bp	
Glucose-6-phosphatase (*G6Pase*)	**FP:** CTGTTTGGACAACGCCCGTAT **RP:** AGGTGACAGGGAACTGCTTTA	56°C	91bp	
Glucose transporter 2 (*GLUT2*)	**FP:** CTTGGAAGGATCAAAGCAATG **RP:** CAGTCCTGAAATTAGCCCAC	60°C	150bp	
Glycogen Synthase (*GS*)	**FP:** ACCAAGGCCAAAACGACAG **RP:** GGGCTCACATTGTTCTACTTG	61°C	102bp	
Glycogen Phosphorylase (*GP*)	**FP:** GAGAAGCGACGGCAGATCA **RP:** CTTGACCAGAGTGAAGTGCA	65°C	102bp	
Sirtuin 1 (*SIRT-1*)	**FP:** GATGAAGTTGACCTCCTCA **RP:** GGGTATAGAACTTGGAATTAG	61°C	86bp	Skeletal muscles (SK)
Peroxisome proliferator-activated receptor gamma coactivator 1-alpha (*PGC-1α*)	**FP:** AGCCGTGACCACTGACAACGA **RP:** GTAGCTGAGCTGAGTGTTGGC	69°C	129bp	
Adipose triglyceride lipase (*ATGL*)	**FP:** CAACGCCACTCACATCTACGG **RP:** GGACACCTCAATAATGTTGGCAC	61.8°C	158bp	Adipose Tissue (AT)
Acetyl-CoA carboxylase 1 (*ACC-1*)	**FP:** ACGCTCAGGTCACCAAAAAGAAT **RP:** GTAGGGTCCCGGCCACAT	57°C	70bp	
Melatonin receptor B (*MTNR1B*)	**FP:** TTGTGATGGGCCTGAGTGTC **RP:** AGCCAGACGAGGCTGATGTA	60°C	145bp	
Glucose transporter 4 (*GLUT4*)	**FP:** TAGGAGCTGAGGGTTGGCTA **RP:** TGCTCCAGTAGGCCGTAAAC	60°C	111bp	
GAPDH	**FP:** AGGTCGGTGTGAACGGATTTG **RP:** TGTAGACCATGTAGTTGAGGT	56°C	123bp	Liver, SK, AT

[FP: Forward Primer; RP: Reverse Primer; bp: base pair]

3.2.7 Glucoregulatory enzyme activity and liver glycogen content:

A portion of the liver tissue was harvested and snaps frozen with dry ice, then stored at -80 °C for enzyme activity assays. 50 mg tissue was homogenized, and tissue lysates were used for the activity assays. Enzyme assays for glucokinase (GCK), fructose-1,6-bisphosphatase (FBPase), phosphoenolpyruvate carboxykinase (PEPCK), glycogen phosphorylase (GP), and glycogen content were carried out by commercially available kits (BioVision, Milpitas, CA, USA) according to the manufacturer's protocol.

3.2.8 Mitochondrial oxygen consumption rate (OCR):

A portion of skeletal muscle was harvested and stored in mitochondrial respiration buffer at -80 °C for the OCR studies. Mitochondria were isolated from skeletal muscle using a mitochondria isolation kit (Thermo Scientific TM, Catalog no. 89801) using the manufacturer's protocol. The isolated mitochondria were resuspended in 100 µl of mitochondria respiration buffer (110mM Sucrose, 0.5mM EGTA, 70 mM KCl, 0.1% FFA free BSA, 20 mM HEPES, 3 mM $MgCl_2$, and 10 mM KH_2PO_4, 20mM Taurine) (Butterick et al, 2016). OCR studies were carried out in an Oxytherm System (Hansatech Instruments Ltd., Pentney, UK). Outer membrane integrity of the isolated mitochondria was evaluated by impermeability to exogenous cytochrome c, which was constantly >95%. The activities of respiratory chain complexes I-IV were monitored using 100 µl of substrates [100 mM Pyruvate & 800 mM Malate (complex I), 1 M Succinate (complex II), 10 mM α-glycerophosphate (complex III), and 0.8 M ascorbate (complex IV)] (Li and Graham, 2012) added to 90 µl of mitochondria suspension. Other respiration reagents used were 100 mM adenosine diphosphate (100 µl), 1 mM oligomycin (2 µl), 1 mM rotenone (1 µl), and 1 mM Antimycin (2.5 µl). Protein concentration was estimated by the Bradford method (Stoscheck et al., 1990). All chemicals were purchased from Sigma-Aldrich, USA. OCR was determined by measuring the amount of oxygen (nmol) consumed, divided by the time elapsed (min) and the amount of protein present in the assay (Li and Graham, 2012). Data is represented as the respiratory control ratio (RCR) of state 3/state 4 respiration.

3.2.9 Western Blot Analysis:

The skeletal muscle was also harvested and stored in the lysis buffer containing protease inhibitor cocktail and phosphatase inhibitor cocktail 2 and 3 (both from Sigma, St. Louis, MO, USA) at -80 °C for western blot analysis of key proteins involved in the insulin signaling pathway. The tissue was homogenized in liquid nitrogen and Laemmli buffer (1M Tris HCl,

10% SDS, 20% glycerol, and 10% β-mercaptoethanol) containing 1 M urea (1:1). The homogenate was collected and sonicated twice in cold conditions and centrifuged to remove tissue/cell debris. After performing the TCA precipitation method, the protein concentration in the lysates was estimated using the Bradford assay (Stoscheck et al., 1990). Total 25-40 µg of the lysates were resolved on 8-10% SDS-PAGE, followed by electrophoretic transfer to the PVDF membrane. Membranes were blocked with 5% bovine serum albumin (Sisco Research Laboratories Pvt. Ltd., Mumbai, MH, India) for phosphorylated proteins and blotting-grade blocker (Bio-Rad) for non-phosphorylated proteins in tris-buffered saline (pH 8.0) with 0.1% Tween-20 for 1 hour at room temperature. For immunoblot analysis, the membrane was incubated overnight with different targeted primary antibodies at 4°C. Membranes were then incubated with secondary antibodies at room temperature for 1 hour. The details of primary and secondary antibodies are shown in Table 3.2. The membrane was visualized with the clarity western ECL substrate (Bio-Rad Laboratories, USA) in the ChemiDoc™ Touch Imaging System. Blots were analyzed in Image LabTM software (Bio-Rad Laboratories, USA).

Table 3.2. List of antibodies used for the immunoblot analysis.

Sr. No.	Primary Antibody	Make
1.	β-actin (1:1000, Mouse)	ABclonal Technology, USA
2.	Insulin Receptor β (1:1000, rabbit)	Cell Signaling Technology, USA
3.	IRS-1 (1:1000, Rabbit)	ABclonal Technology, USA
4.	pIRS-1 Ser307 (1:1000, Rabbit)	Cell Signaling Technology, USA
5.	Akt-1 (1:1000, Rabbit)	ABclonal Technology, USA
6.	pAkt-1 S473 (1:1000, Rabbit)	ABclonal Technology, USA
7.	Glut-4 (1:1000, Rabbit)	ABclonal Technology, USA
8.	Anti-mouse IgG-HRP (1:10000, goat)	Genei, Bangalore
9.	Anti-rabbit IgG-HRP (1:5000, goat)	Jackson ImmunoResearch, USA

3.2.10 Immunohistochemistry-immunofluorescence (IHC-IF) analysis:

The pancreas was fixed in 10% neutral buffered formalin for histological processing and paraffin embedding. 5µm sections were prepared from the paraffin-embedded blocks. Immunofluorescence staining was carried out to study β-cell mass and islet number (Insulin staining). The sections were deparaffinized in xylene and rehydrated in a series of graded ethanol (100%, 95%, 80%, and 70%). Antigen retrieval was performed using 1N HCl for 45 minutes at 37 °C. Sections were blocked in 5% donkey serum in PBST (PBS + 0.1% Tween 20) for 1 hour at room temperature and incubated with primary antibody prepared in blocking

buffer at 37 °C in a humidified chamber for 2 hours (guinea pig anti-insulin ; 1:200). Tissue sections were washed with PBS and incubated with secondary antibodies at room temperature for 45 minutes in the dark (donkey anti-guinea pig Alexa Fluor 488; 1:500). Tissue sections were washed with PBS and distilled water, and were mounted with Slowfade Gold Antifade mountant with DAPI (Thermo Fisher Scientific, USA), and the coverslip was sealed with nail varnish. Whole stained pancreatic tissue section images were acquired on the tile-scan mode (with automatic image stitching) under a laser scanning microscope (Leica SP8 TCS, Mannheim, Germany) at 10X magnification for β-cell mass & islet number, and image analyses was carried out in Image J software. Observations were made from three pancreatic sections per group. The β-cell mass (mg/pancreas) was calculated as insulin-positive area/total pancreas area x pancreas weight.

3.2.11 Statistical Analyses:

Statistical data comparisons were performed by one-way analysis of variance (ANOVA) and multiple group comparisons by Tukey's post hoc test in Graphpad Prism 6 (GraphPad Sofware, San Diego, CA, USA). The significance level was set at $p<0.05$. Results are expressed as mean±SEM.

3.3 Results

3.3.1 Assessment of metabolic profile:

Our results suggested that monotherapies (M, $p<0.01$; G, $p<0.01$) are as effective as combination therapy ($p<0.001$) in reducing FBG levels, increasing glucose tolerance (S, $p<0.01$; M, $p<0.05$; M+G, $p<0.001$) and insulin sensitivity (S, $p>0.05$; M, $p>0.01$; S+M, $p<0.001$). The BW of the HFD group was significantly increased compared to the NCD group ($p<0.001$). However, the drug-treated groups did not significantly reduce the final BW compared to their initial BW ($p>0.05$). Moreover, an assessment of food and water intake revealed that there was a significant reduction in food intake (HFD, $p<0.05$; M, M+G; $p<0.01$), and no difference was observed for the water intake (HFD, M, G, M+G; $p>0.05$) in the drug-treated and HFD groups as compared to NCD group. Further, a notable change in water intake was observed before and after treatment in M+G treated group ($p<0.05$) (Figure 3.1A-F).

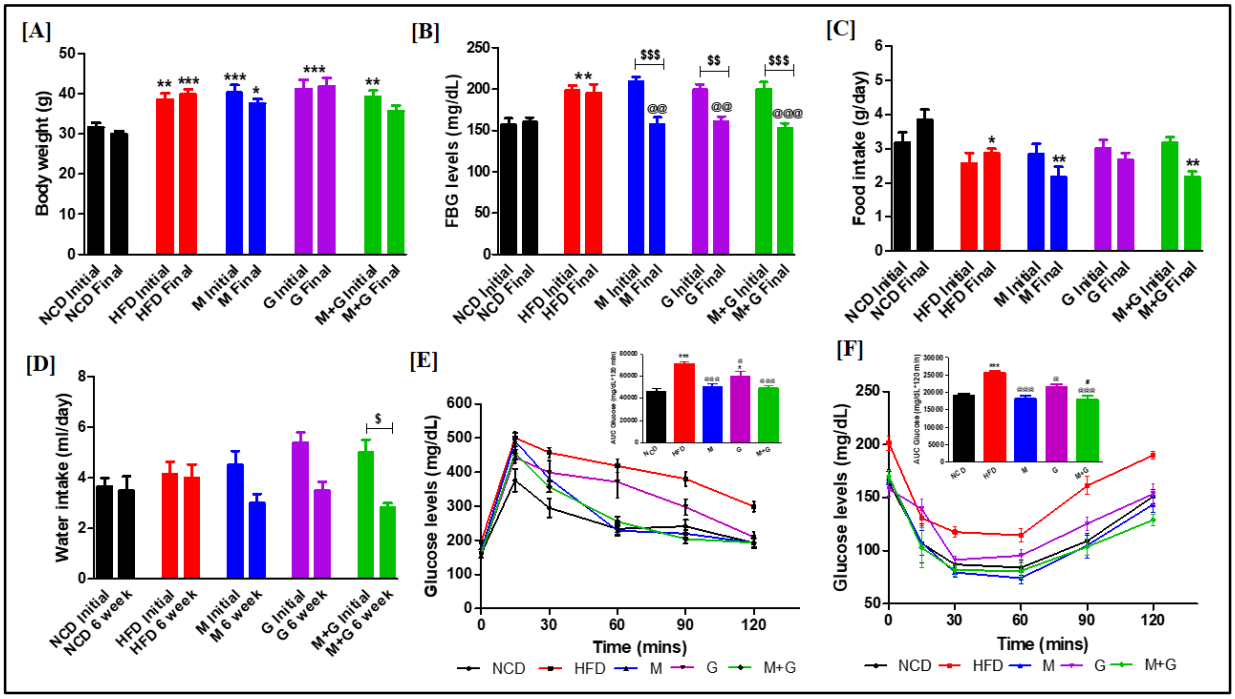

Figure 3.1. Evaluation of bodyweight, blood glucose levels, food and water intake, IPGTT and IPITT. [A] Bodyweight: A significant increase in body weight was observed in HFD group compared to NCD group. No significant difference was observed in the body weight of drug-treated groups. **[B] Fasting blood glucose levels:** A significant increase in FBG levels was observed in HFD group and reduction in all the drug-treated groups. **[C] Food intake:** No significant difference was observed in the food intake post-drug treatment. HFD-fed and other drug-treated groups showed a reduction in food intake as compared to NCD group. [**D] Water intake:** A significant reduction in water intake was observed in M+G treated group post-drug treatment. **[E] lPGTT and AUC glucose curve:** Increased glucose clearance was observed in all the treated groups compared to HFD-fed mice. **Blood glucose AUC0–120:** All the treated groups showed a significant increase in glucose tolerance compared to HFD-fed mice. **[F] lPITT and AUC glucose curve:** Increased glucose clearance was observed in all the treated groups compared to HFD-fed mice. **Blood glucose AUC0–120:** All the treated groups showed a significant increase in insulin sensitivity compared to HFD-fed mice. (*p<0.05, **p<0.01, ***p<0.001 vs. NCD; $^{@}p$<0.05, $^{@@}p$<0.01, $^{@@@}p$<0.001 vs. HFD; $^{\#}p$<0.05 vs. GABA) (n=6-8/group).

3.3.2 Assessment of plasma lipid profile, and insulin, leptin & melatonin levels:

Analysis of plasma lipid profile suggested that the levels of HDL were elevated in the HFD group but were not significant; however, TG, TC, and LDL levels were significantly increased in the HFD group (TG, p<0.001; TC, p<0.01; LDL, p<0.05) as compared to NCD, indicating dyslipidemia. Lipid levels (TG, TC, and LDL) were restored in all the drug-treated groups as compared to the HFD group (TG: M, G, M+G, p<0.001; TC: M, p<0.01; G, M+G, p<0.01;

LDL; M, G, M+G, $p<0.01$). However, no changes in HDL levels were observed in any of the drug-treated groups ($p>0.05$). Furthermore, analysis of plasma insulin, leptin, and melatonin levels revealed that there was hyperinsulinemia and hyperleptinemia along with the decreased melatonin levels in the HFD group as compared to NCD ($p<0.001$), and the levels were restored in the drug-treated groups (insulin: M, M+G, $p<0.01$; G, $p<0.05$; leptin: M, M+G, $p<0.05$; melatonin: M, M+G, $p<0.001$) as compared to HFD group (Figure 3.2A-G).

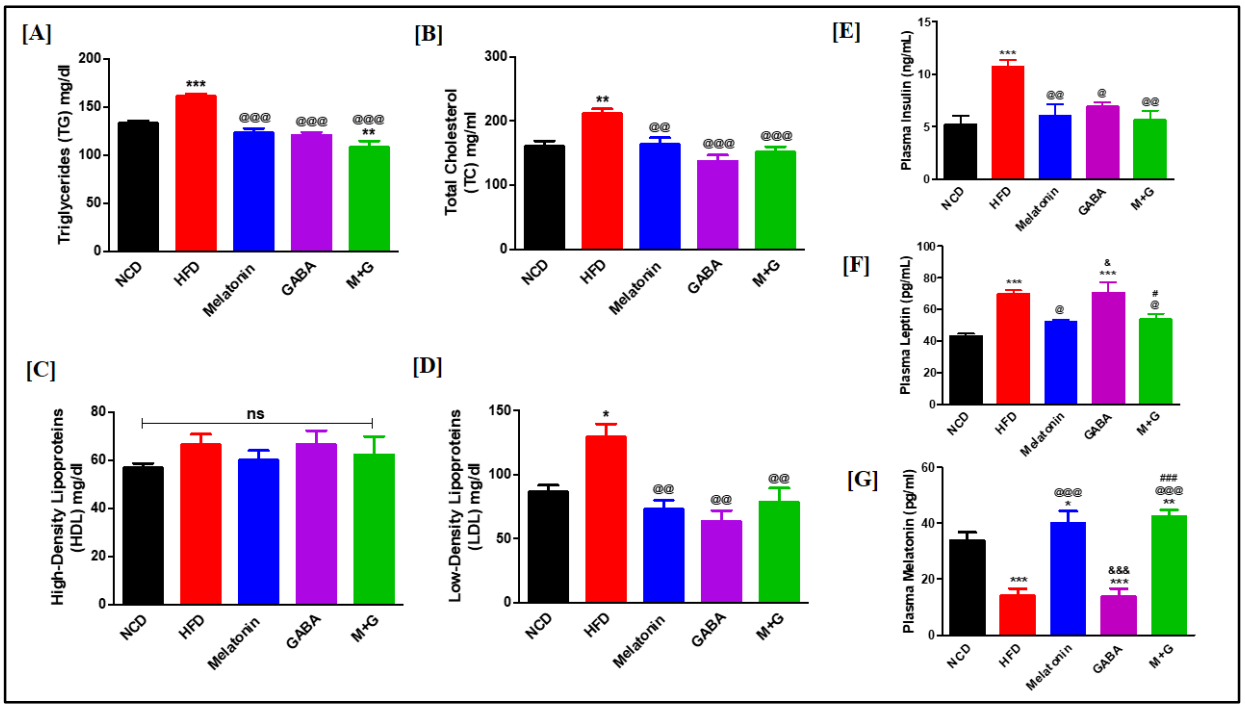

Figure 3.2. Evaluation of plasma lipid profile, insulin, leptin, and melatonin levels. A significant reduction of: **[A]** triglycerides, **[B]** total cholesterol, and **[D]** LDL was observed in all the drug-treated groups as compared to HFD group. **[C]** In comparison, HDL levels were non-significant. **[E] Fasting plasma insulin levels:** A significant reduction in plasma insulin was observed in all the drug-treated groups compared to HFD group. **[F] Fasting plasma leptin levels:** A significant reduction in plasma leptin was observed in M & M+G treated groups compared to HFD-fed mice. **[G] Fasting plasma melatonin levels:** A significant increase in plasma melatonin was observed in M & M+G treated groups compared to HFD-fed mice. (*$p<0.05$, **$p<0.01$, ***$p<0.001$ vs. NCD; $^{@}p<0.05$, $^{@@}p<0.01$, $^{@@@}p<0.001$ vs. HFD; $^{\&}p<0.05$, $^{\&\&\&}p<0.001$ vs. Melatonin; $^{\#}p<0.05$, $^{\#\#\#}p<0.001$ vs. GABA) (n=5-6/group).

3.3.3 Assessment of key glucoregulatory enzyme gene expression & specific activity, and liver glycogen content:

GCK enzyme activity was significantly increased in the M+G group ($p<0.05$) as compared to the HFD group indicating increased glucose uptake. *G6Pase* expression was significantly reduced in all the drug-treated groups (M, G, $p<0.05$; M+G, $p<0.01$) as compared to the HFD

group, indicating increased glucose uptake, and *GLUT2* expression was significantly reduced in GABA and M+G groups (G, M+G, $p<0.05$) as compared to HFD group. Furthermore, the gene expression and activity of FBPase and PEPCK were significantly increased in the HFD group ($p<0.05$ and $p<0.01$, respectively) as compared to NCD group, and significantly reduced in M ($p<0.05$) & M+G ($p<0.01$) and G & M+G groups ($p<0.05$), respectively, suggesting the reduced gluconeogenesis. Additionally, there was a significant reduction in the gene expression (M, $p<0.05$; G, $p<0.05$; M+G, $p<0.05$) and activity of GP (M, $p<0.001$; G, $p<0.01$; M+G, $p<0.001$) in all the drug-treated groups as compared to HFD group, indicating reduced glycogenolysis. No significant change in *GS* expression was observed in any of the drug-treated groups ($p>0.05$) compared to HFD group. However, elevated glycogen content in all the drug-treated groups (S, M, S+M, $p<0.001$) indicated an increase in glycogenesis (Figure 3.3A-L).

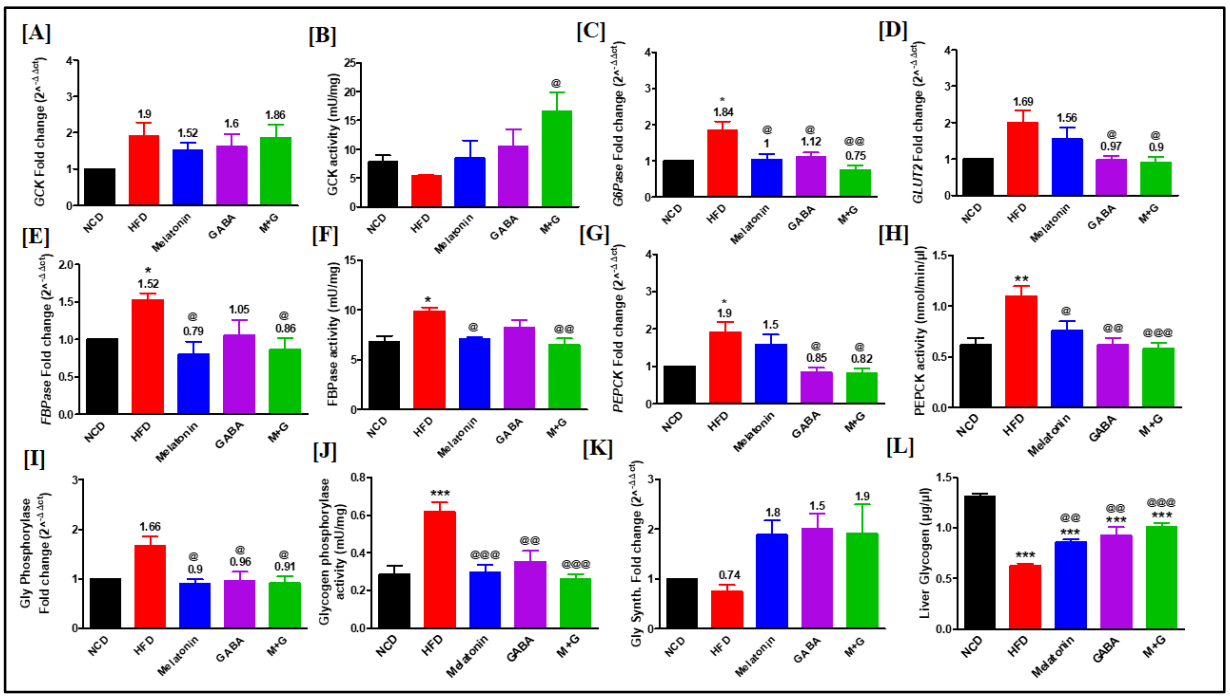

Figure 3.3. Gene expression and enzyme activities of glucoregulatory enzymes and glycogen content in the liver. [A-B] GCK mRNA fold-change and activity. No significant change in *GCK* expression was observed in any of the drug-treated groups compared to HFD group. Intriguingly, its activity was significantly increased in M+G treated group. **[C] G6Pase mRNA fold change:** *G6Pase* expression was significantly increased in HFD group, whereas it was reduced significantly in all the drug-treated groups. **[D] GLUT2 mRNA fold change:** A significant reduction in *GLUT2* expression was observed in the G and M+G treated groups as compared to HFD group. **[E-F] FBPase mRNA fold-change and its activity:** *FBPase* gene expression and its activity were significantly increased in HFD, whereas in the M and M+G treated groups, it was reduced significantly. **[G-**

H] PEPCK mRNA fold-change and activity: *PEPCK* expression and activity were significantly increased in HFD group. In contrast, its fold change was significantly decreased in the G and M+G treated groups, and its activity was decreased in all the drug-treated groups. **[I-J] GP mRNA fold-change and activity:** All the drug-treated groups showed a significant decrease in GP expression and activity. **[K] GS mRNA fold change:** No significant change in *GS* expression was observed in any of the drug-treated groups as compared to HFD group. **[L] Liver glycogen content (GC):** GC was significantly reduced in HFD group, whereas it was increased significantly in all the drug-treated groups. (*p<0.05, **p<0.01, ***p<0.001 vs. NCD; $^{@}p$<0.05, $^{@@}p$<0.01, $^{@@@}p$<0.001 vs. HFD) (n=5-6/group).

3.3.4 Gene expression analysis of mitochondrial biogenesis markers in skeletal muscle and lipid metabolism markers, *MTNR1B,* & *GLUT4* in Adipose Tissue:

Expression of crucial markers for mitochondrial biogenesis, i.e., *Sirtuin 1* (*SIRT1)* and *Peroxisome proliferator-activated receptor gamma coactivator 1-alpha* (*PGC1α),* showed a significant increase in all the drug-treated groups as compared to HFD group (SIRT1: G, p<0.01; M, M+G, p<0.001; PGC1α: M, G, p<0.05; M+G, p<0.01). Lipid metabolism markers, i.e., *Acetyl-CoA carboxylase* 1 (*ACC1)* expression was reduced in both HFD and the drug-treated groups (M, G, M+G, p<0.001), whereas *Adipose triglyceride lipase* (*ATGL)* expression was significantly reduced in all the drug-treated groups (G, p<0.05; M, M+G, p<0.001) as compared to HFD group, suggesting the improved lipid metabolism (Figure 3.4A-D). Additionally, we studied absolute gene expression of *MTNR1B* and *GLUT4* in adipose tissue by ddPCR. The results show an increased copy number/µl of the mentioned genes in the HFD group as compared to the NCD group, suggestive of the insulin resistance in mice. In contrast, the copy number/µl of *MTNR1B* and *GLUT4* were reduced in all the drug-treated groups, suggestive of the reduced insulin resistance (Figure 3.4E-F).

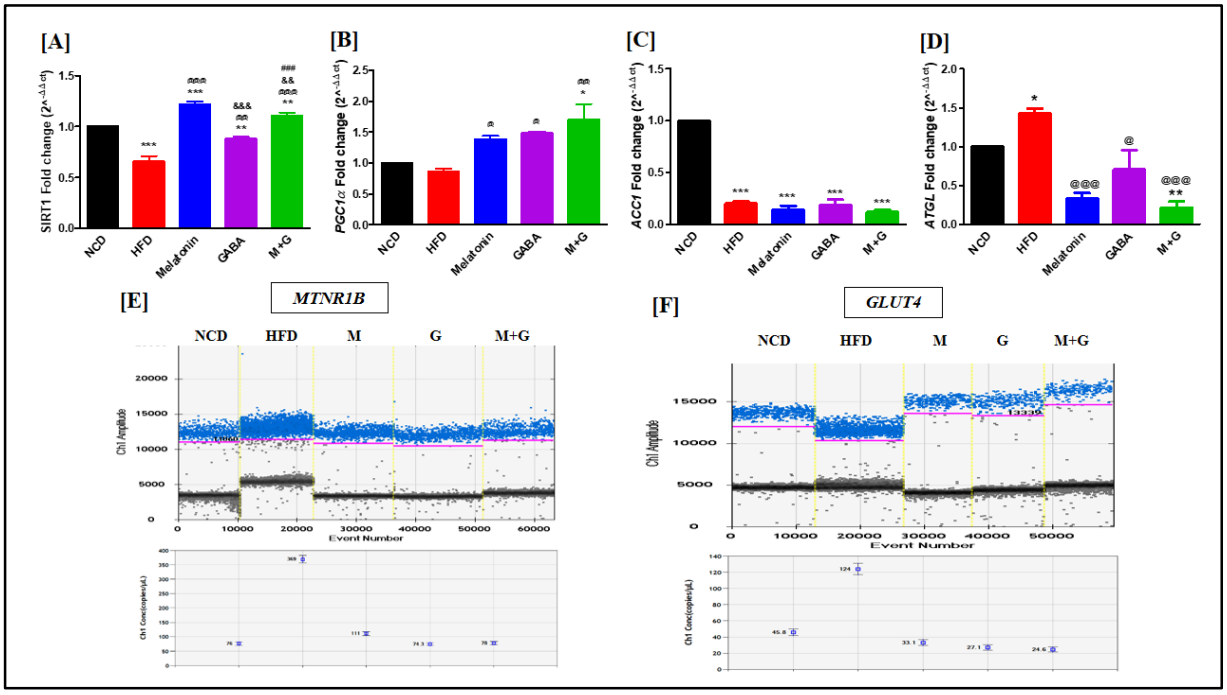

Figure 3.4. Gene expression of mitochondrial biogenesis markers in skeletal muscle, lipid metabolism markers, and absolute gene quantification of *MTNR1B* and *GLUT4* in adipose tissue. [A-B] mRNA fold change of *SIRT1* and *PGC1a* in skeletal muscle: A significant reduction in *SIRT1* mRNA levels was observed in HFD group, whereas all the drug-treated groups showed a significant increase in *SIRT1* and *PGC1a* expression. **[C-D] mRNA fold change of *ACC1* and *ATGL* in adipose tissue:** There was no change in *ACC1* expression, whereas a significant reduction in *ATGL* gene expression was observed in all the drug-treated groups as compared to HFD. **[E-F] Absolute gene quantification of *MTNR1B* and *GLUT4* in the adipose tissue:** Gene expression of *MTNR1B* and *GLUT4* was higher in the HFD group as compared to the NCD group. In contrast, it was reduced in all the drug-treated groups as compared to the HFD groups, and it is represented by a change in amplitude of positive droplets (blue) and the number of copies/µl. Blue droplets: positive for the target gene; Grey droplets: negative for the target gene; Pink line: threshold intensity to discriminate positive and negative droplets (n=3/group). (*p<0.05, **p<0.01, ***p<0.001 vs. NCD; $^{@}p$<0.05, $^{@@}p$<0.01, $^{@@@}p$<0.001 vs. HFD; $^{\&\&}p$<0.01, $^{\&\&\&}p$<0.001 vs. Melatonin; $^{\#\#\#}p$<0.001 vs. GABA) (n=6-8/group).

3.3.5 Estimation of mitochondrial respiratory control ratio (RCR) of complexes I-IV in skeletal muscle:

The RCR of state 3/state 4 for mitochondrial complexes I, II, III, and IV (p<0.001, p<0.001, p<0.01, & p<0.05, respectively) was significantly reduced in the HFD group as compared to NCD group.

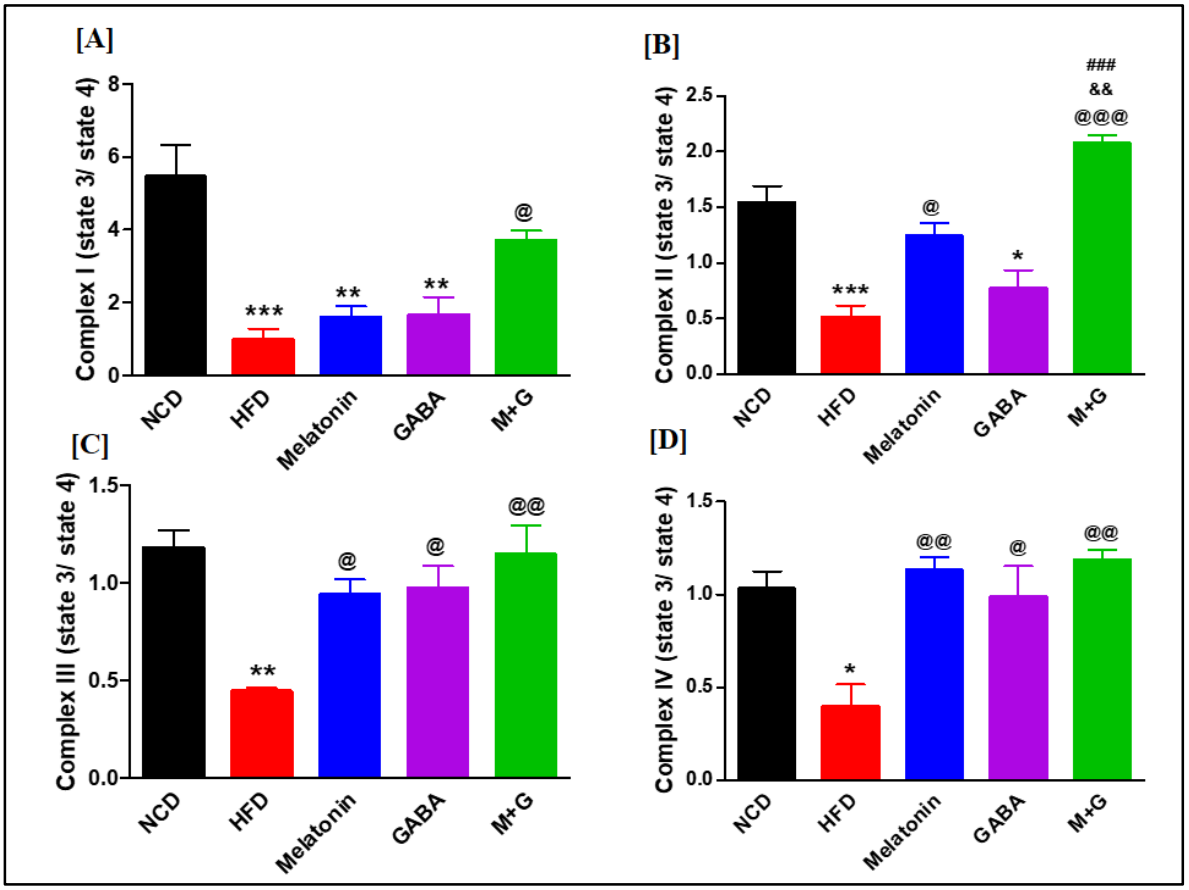

Figure 3.5. Mitochondrial respiratory control ratio (state 3/state 4) in the skeletal muscle. [A] Complex I: RCR was significantly reduced in the HFD group as compared to NCD group and was significantly increased in the M+G treated group **[B] Complex II:** RCR was reduced significantly in the HFD group compared to NCD group and was increased significantly in the M and M+G treated groups. **[C-D] Complex III-IV:** RCR was significantly reduced in the HFD group compared to NCD group and increased significantly in all the drug-treated groups. (*p<0.05, **p<0.01, ***p<0.001 vs. NCD; $^{@}p$<0.05, $^{@@}p$<0.01, $^{@@@}p$<0.001 vs. HFD; $^{\&\&}p$<0.01 vs. Melatonin; $^{\#\#\#}p$<0.001 vs. GABA) (n=3/group).

Further, a significant increase in the RCR was observed in all the drug-treated groups for CIII (M, p<0.05; G, p<0.05; M+G, p<0.01) and CIV (M, p<0.01; G, p<0.05; M+G, p<0.01). However, the RCR of state 3/state 4 for CI was significantly increased only in the M+G (p<0.05) and for CII in M (p<0.05) and M+G (p<0.001) treated groups (Figure 3.5A-D).

3.3.6 Protein expression analysis for insulin signaling pathway in skeletal muscle:

Western blot analysis of key proteins involved in the insulin signaling pathway showed that insulin receptor-β (IR1β) (p<0.05), pAkt Ser473/Akt (p<0.05), and GLUT4 (p<0.05) levels were significantly downregulated in HFD group, while pIRS Ser307/IRS (p<0.05) levels

significantly upregulated in HFD group (p<0.05) as compared to NCD group, which is suggestive of peripheral insulin resistance.

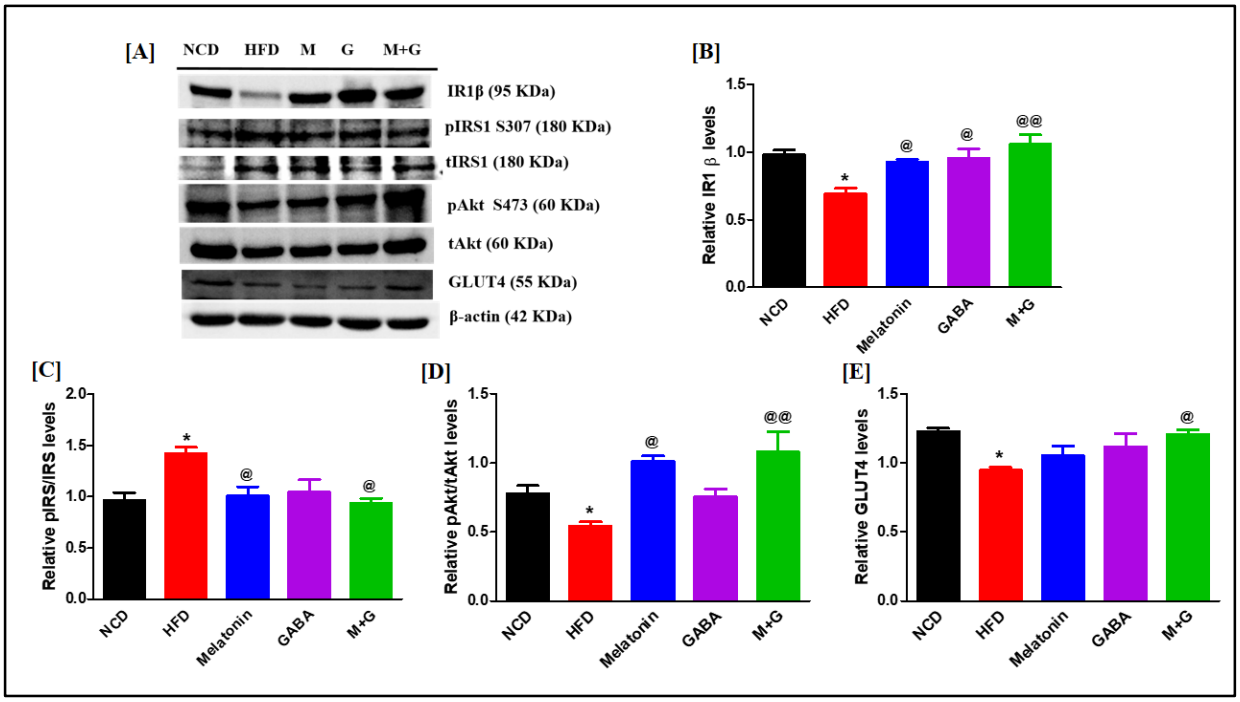

Figure 3.6 Protein expression of the insulin signaling pathway in skeletal muscle. [A] Representative western blot images. **[B] Insulin Receptor 1β:** IR1β protein expression was significantly reduced in HFD group as compared to NCD group, whereas all the drug-treated groups showed a significant increase in IR1β. **[C] pIRS/IRS:** pIRS/IRS levels were significantly increased in HFD and were reduced significantly in M and M+G treated groups. **[D] pAkt/Akt:** pAkt/tAkt levels were significantly decreased in HFD group while increasing significantly in the M and M+G treated groups. **[E] GLUT4:** GLUT4 protein expression was significantly decreased in the HFD group, while increasing significantly in the M+G treated group. (*p<0.05 vs. NCD; $^{@}p$<0.05, $^{@@}p$<0.01 vs. HFD) (n=4/group).

In the drug-treated groups, there was an upregulation of IR1β (M, p<0.05; G, p<0.05; M+G, p<0.01), and pAkt/Akt levels (M, p<0.05; M+G, p<0.01), as compared to HFD group. Moreover, the levels of pIRS/IRS were significantly downregulated in M and M+G groups (M, p<0.05; M+G, p<0.05), suggestive of the improved insulin sensitivity. Intriguingly, GLUT4 levels were significantly upregulated only in M+G treated groups (p<0.05) as compared to the HFD group (Figure 3.6A-E).

3.3.7 Assessment of β-cell mass and islet number in pancreas:

Immunohistochemistry (IHC) analysis of the pancreatic tissue showed that β-cell mass was significantly increased in the HFD group as compared to NCD (p<0.001). All the drug-treated

groups (G, $p<0.01$; M, M+G, $p<0.001$) showed a significant decrease in β-cell mass compared to the HFD group. Intriguingly, the islet number per pancreatic section was also significantly increased in the HFD group ($p<0.001$) as compared to NCD; however it was notably reduced in all the drug-treated groups (M, G, M+G, $p<0.001$) as compared to HFD group, revealing a reduction in β-cell hyperplasia and hypertrophic condition as shown in Figure 3.7A-C.

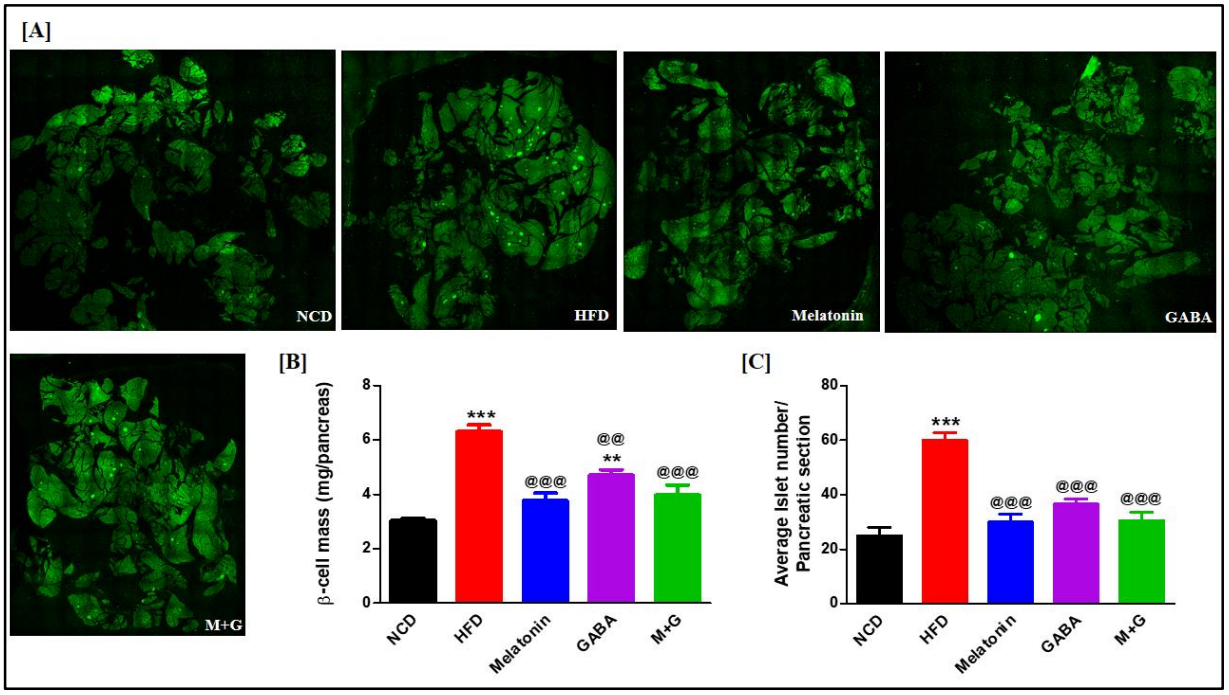

Figure 3.7. Pancreatic β-cell mass and islet number. [A] Immunofluorescence staining for insulin (green) in mouse pancreatic tissue. **[B] Pancreatic β-cell mass:** β-cell mass was significantly increased in the HFD group, while it was reduced significantly in all the drug-treated groups as compared to the HFD group. **[C] Islets Number per pancreatic section:** Islet number was significantly increased in the HFD group as compared to the NCD group, while it was reduced significantly in all the drug-treated groups as compared to the HFD group. Magnification- 10X. (**$p<0.01$, ***$p<0.001$ vs. NCD; $^{@@}p<0.01$, $^{@@@}p<0.001$ vs. HFD) (n=3/group).

3.4 Discussion:

T2D is a metabolic disorder associated with a disturbed circadian rhythm and reduced melatonin levels (Scheer et al., 2009). The pathophysiology of T2D is more complex and multifaceted and involves several factors, including abnormalities in insulin secretion, insulin resistance, leptin resistance, metabolic and mitochondrial dysfunction, and a gradual loss of β-cell mass and function. In chapter 2, we demonstrated the effect of melatonin administration combined with GABA in ameliorating T1D in mouse models by promoting β-cell regeneration. Here, we sought to investigate the potential beneficial effects of melatonin administration

combined with GABA, in the amelioration of T2D manifestations in a mouse model. Our findings demonstrate that monotherapies and combination therapy can enhance glycolipid metabolism in the liver and adipose tissue and elevate mitochondrial activity in skeletal muscle. They can also reduce hyperglycemia, hyperinsulinemia, hyperleptinemia, and dyslipidemia. Additionally, it restored peripheral insulin sensitivity, β-cell mass, and islet number in T2D mice.

Melatonin is a pleiotropic hormone that regulates metabolic activities by acting on MTNR1A and MTNR1B receptors in central and peripheral tissues. These are G protein-coupled receptors, and most signaling pathways depend on Gi proteins, which inhibit the protein kinase A (PKA) - cAMP response element-binding protein (CREB) pathway. It also inhibits ion channels, including Kir3 and large-conductance Ca^{2+}-activated potassium channels (BKCa), as well as other kinases, such as protein kinase G (PKG), protein kinase C (PKC), phosphoinositide 3-kinase (PI3K), Akt, and extracellular-signal-regulated kinase (ERK) (Cecon et al., 2018). On the other hand, melatonin promotes the Gq-PKC-phospholipase C (PLC) pathway, which enhances the insulin release (Oishi et al., 2018). In addition to the pineal gland, the retina, pancreas, adipose tissue, and liver are some of the tissues that locally produce melatonin. Shieh et al. (2009) demonstrated that melatonin can promote glycogen synthesis in HepG2 cells by activating protein kinase C, zeta (PKCζ), Akt, and glycogen synthase kinase-3β (GSK3β), besides impeding gluconeogenesis in rats (Poon et al., 2001). Further studies have demonstrated that melatonin regulates glucose metabolism by elevating PI3K-Akt activity (Tuomi et al., 2016; Brydon et al., 2001) corroborate our findings. Furthermore, studies have shown that melatonin can activate the IRS1-PI3K-PKC pathway, which promotes glucose uptake in mouse skeletal muscle cells, but this effect is attenuated in MT1 knockout mice (Owino et al., 2018). Furthermore, melatonin has been found to inhibit the cAMP-PKA pathway, thereby preventing lipolysis and fatty acid transport in rat adipocytes (Zalatan et al., 2001). Brydon et al. (2001) observed that melatonin has distinct effects on adipose tissue depending on whether it is administered acutely or chronically. In acute treatment, melatonin inhibits the production of cAMP and cGMP in PAZ6 human brown adipocyte cell line, while in chronic treatment, it reduces GLUT4 expression and glucose uptake (Brydon et al., 2001). In various experimental models, melatonin decreases body weight and white adipose tissue in rodents (Cipolla-Neto et al., 2014). However, some small-scale clinical studies of melatonin

administration revealed a negligible effect on body weight loss while having the opposite results on plasma lipids (Karamitri and Jockers, 2019). Clinical experiments with acute melatonin treatment demonstrated an impaired glucose tolerance (Rubio-Sastre et al., 2014; Cagnacci et al., 2001). However, chronic melatonin treatment for up to five months showed reduction in HbA1c levels and hyperglycemia (Garfinkel et al., 2011). These reports support our findings. A recent meta-analysis of randomized clinical trials investigating the effects of melatonin supplementation on diabetes patients has suggested that it reduces FBG, HbA1c levels, and insulin resistance (Delpino et al., 2021). Moreover, our recent study has also suggested that melatonin in combination with sitagliptin ameliorates T2D manifestations and preserves the β-cell mass *in vitro* and *in vivo* (Patel et al., 2023).

GABA acts as a growth factor for pancreatic endocrine cells through autocrine (Braun et al., 2010; Gammelsaeter, 2004) and paracrine (Taneera et al., 2012; Braun et al., 2004), signaling to enact its involvement in the regulation of hormone secretion from islet cells (Braun et al., 2012). GABA via $GABA_AR$ and $GABA_BR$ promotes the phosphorylation of CREB (cAMP response element-binding protein) (Purwana et al., 2014), a key transcription factor responsible for the maintenance of insulin gene transcription and β-cell survival in rodent and human islets (Shao et al., 2013). Among targets of CREB, the insulin receptor substrate-2 gene (IRS-2) is crucial in regulating β-cell mass and function (Purwana et al., 2014). Apart from the pancreas, the GABAergic system functions in many peripheral tissues like the pancreas and liver. $GABA_AR$ regulates PI3K/Akt activities in the liver that maintain hepatocyte survival and PGC-1α expression. Thus, GABA is one of the factors responsible for regulating the hepatic glucose metabolism, i.e., gluconeogenic and glycogenolytic pathways (Wang et al., 2017). Fibroblast growth factor 21 (FGF-21), predominantly expressed in the liver under normal conditions induces PGC-1α expression, leading to the regulation of lipolysis in the adipose tissue and thereby forming liver-adipose tissue crosstalk (Ye et al., 2017). Choi et al. (2016) reported that GABA-enriched fermented sea tangle promotes brain-derived neurotrophic factor-mediated muscle growth and lipolysis in middle-aged women. Previously, it has been reported that T2D subjects have impaired mitochondrial TCA cycle flux in skeletal muscle (Gaster et al., 2012; Befroy et al., 2007). In a series of enzymatic reactions, the TCA cycle generates the reducing equivalents NADH and FADH2, which are required to transfer electrons to the mitochondrial respiratory chain (Martínez-Reyes et al., 2020). It could be one possible

reason for impaired mitochondrial respiration in T2D conditions. Increased PGC1α activates branched-chain amino acid metabolism, fatty acid oxidation, and TCA cycle in the skeletal muscle (Hatazawa et al., 2014, 2018; Lira et al., 2010). We found that GABA treated group showed an increase in *SIRT1* and *PGC1α* expression and improved mitochondrial respiratory control ratio (RCR) of complexes I-IV in skeletal muscle. Thus, GABA could improve mitochondrial biogenesis and oxygen consumption rate, possibly by regulating SIRT1 and PGC1α, which might also ameliorate skeletal muscle's insulin resistance.

Interestingly, our study also reveals increased glycolysis, glycogen synthesis, and glycogen content and reduced gluconeogenesis, glycogenolysis, and *GLUT2* expression in the liver, suggesting the improved glucose metabolism in the liver in all the drug-treated groups. We also observed a decrease in *ATGL* (lipolytic) transcript levels in adipose tissue with no change in *ACC1* (lipogenic) in all the drug-treated groups. In addition, increased *SIRT1* and *PGC1-α* (mitochondrial biogenesis genes) transcript levels in the skeletal muscle indicate an improved lipid metabolism and insulin sensitivity in the respective tissues. Our mitochondrial studies suggested increased respiratory chain complexes I-IV activities in the skeletal muscle of all the drug-treated groups, presumably by improving *SIRT1* and *PGC1-α* levels upon drug treatment. Atkinson et al. (2013) reported that overexpression of *GLUT4* increases insulin sensitivity and glucose tolerance in HFD-fed mice (Atkinson et al., 2013), and its expression changes with short-term and long-term HFD feeding (Kim et al., 2014). In support of these studies, our ddPCR results revealed an increased expression of *MTNR1B* and *GLUT4* in the HFD group, indicating the insulin resistance. In contrast, their levels in the adipose tissue of all the drug-treated groups were restored. It is possible that the overexpression might occurred to compensate for insulin resistance in the HFD group, which was then restored in the treatment groups, suggestive of the increased insulin sensitivity. In addition, it was reported that *MTNR1B* overexpression in the adipose tissue leads to increased lipid levels and adipocytes (Brydon et al., 2001), and our findings support these results by showing increased TG levels and fat in the HFD group, while we observed restored expression of *MTNR1B* expression and lipid levels in the drug-treated groups. Moreoevr, over-nutrition causes mTOR/S6K1 signaling activation and it impairs the insulin signaling by increased serine phosphorylation of IRS1 (Jia et al., 2014; Copps and White, 2012). We report a significant decrease in serine phosphorylation of IRS1 and an increase in IR1β, pAKT, and GLUT4 expression in all drug-

treated groups, suggesting an improved insulin signaling pathway in the skeletal muscle.

Thus, we conclude that the melatonin and GABA monotherapies are as effective as combination therapy in ameliorating HFD-induced T2D manifestations by improving glycolipid metabolism, insulin sensitivity, mitochondrial respiration and biogenesis, and restoring β-cell mass (Fig. 3.8). Additionally, species variations and dosage can significantly influence melatonin's effects on glucose homeostasis. Further, to explore the therapeutic potential of melatonin in combination with GABA in clinical studies, it is essential to consider the duration and dosage of melatonin besides the relative timing of its intake, concerning the glycemic challenge.

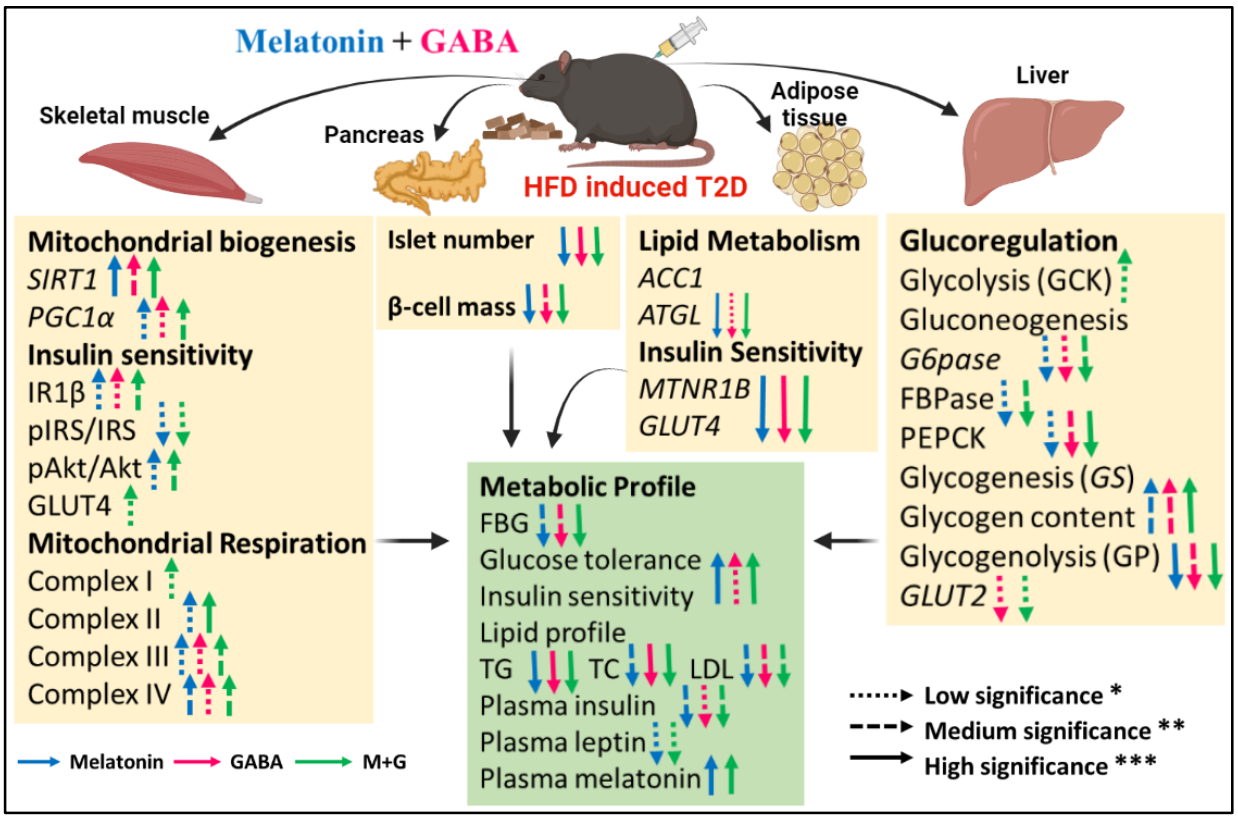

Figure 3.8. Effect of melatonin, GABA, and combination therapy in amelioration of HFD-induced T2D manifestations in a mouse model. Monotherapies are as effective as combination therapy in improving glycolipid metabolism in the liver and adipose tissue, respectively; regulating mitochondrial biogenesis and mitochondrial respiration in the skeletal muscle; increasing insulin sensitivity in the skeletal muscle and adipose tissue; and restoring β-cell mass and islet number in the pancreas. These altogether synergistically restore glucose homeostasis, and ultimately alleviate the T2D symptoms.

3.5 References:

Atkinson BJ, Griesel BA, King CD, Josey MA, Olson AL. Moderate GLUT4 overexpression improves insulin sensitivity and fasting triglyceridemia in high-fat diet–fed transgenic mice. Diabetes. 2013;62(7):2249-58.

Befroy DE, Petersen KF, Dufour S, Mason GF, de Graaf RA, Rothman DL, et al. Impaired mitochondrial substrate oxidation in muscle of insulin-resistant offspring of type 2 diabetic patients. Diabetes. 2007;56(5):1376-81.

Braun M, Ramracheya R, Bengtsson M, Clark A, Walker JN, Johnson PR, et al. γ-Aminobutyric acid (GABA) is an autocrine excitatory transmitter in human pancreatic β-cells. Diabetes. 2010;59(7):1694-701.

Braun M, Ramracheya R, Rorsman P. Autocrine regulation of insulin secretion. Diabetes, Obesity and Metabolism. 2012;14:143-51.

Braun M, Wendt A, Birnir B, Broman J, Eliasson L, Galvanovskis J, et al. Regulated exocytosis of GABA-containing synaptic-like microvesicles in pancreatic β-cells. The Journal of general physiology. 2004;123(3):191-204.

Brydon L, Petit L, Delagrange P, Strosberg AD, Jockers R. Functional expression of MT2 (Mel1b) melatonin receptors in human PAZ6 adipocytes. Endocrinology 2001;142(10):4264-4271.

Cagnacci A, Arangino S, Renzi A, et al. Influence of melatonin administration on glucose tolerance and insulin sensitivity of postmenopausal women. Clinical endocrinology. 2001;54(3):339-346.

Cecon E, Oishi A, Jockers R. Melatonin receptors: molecular pharmacology and signalling in the context of system bias. British journal of pharmacology. 2018;175(16):3263-3280.

Choi WC, Reid SN, Ryu JK, Kim Y, Jo YH, Jeon BH, et al. Effects of γ-aminobutyric acid-enriched fermented sea tangle (Laminaria japonica) on brain derived neurotrophic factor-related muscle growth and lipolysis in middle aged women. Algae. 2016;31(2):175-87.

Cipolla-Neto J, Amaral FG, Afeche SC, Tan DX, Reiter RJ. Melatonin, energy metabolism, and obesity: a review. Journal of pineal research. 2014;56(4):371-381.

Copps KD, White MF. Regulation of insulin sensitivity by serine/threonine phosphorylation of insulin receptor substrate proteins IRS1 and IRS2. Diabetologia. 2012;55(10):2565-82.

Delpino FM, Figueiredo LM, Nunes BP. Effects of melatonin supplementation on diabetes: a systematic review and meta-analysis of randomized clinical trials. Clinical Nutrition.

2021;40(7):4595-4605.

Gammelsaeter R, Frøyland M, Aragón C, Danbolt NC, Fortin D, Storm-Mathisen J, et al. GABA and their transporters in pancreatic islets of Langerhans: evidence for a paracrine transmitter interplay. Journal of cell science. 2004;117(17):3749-58.

Garfinkel D, Zorin M, Wainstein J, Matas Z, Laudon M, Zisapel N. Efficacy and safety of prolonged-release melatonin in insomnia patients with diabetes: a randomized, double-blind, crossover study. Diabetes, metabolic syndrome and obesity: targets and therapy. 2011;4:307.

Gaster M, Nehlin JO, Minet AD. Impaired TCA cycle flux in mitochondria in skeletal muscle from type 2 diabetic subjects: marker or maker of the diabetic phenotype?. Archives of physiology and biochemistry. 2012;118(3):156-89.

Hatazawa Y, Qian K, Gong DW, Kamei Y. PGC-1α regulates alanine metabolism in muscle cells. PloS one. 2018;13(1):e0190904.

Hatazawa Y, Tadaishi M, Nagaike Y, Morita A, Ogawa Y, Ezaki O, et al. PGC-1α-mediated branched-chain amino acid metabolism in the skeletal muscle. PloS one. 2014;9(3):e91006.

Jia G, Aroor AR, Martinez-Lemus LA, Sowers JR. Overnutrition, mTOR signaling, and cardiovascular diseases. American Journal of Physiology-Regulatory, Integrative and Comparative Physiology. 2014;307(10):R1198-206.

Karamitri A, Jockers R. Melatonin in type 2 diabetes mellitus and obesity. Nature Reviews Endocrinology. 2019;15(2):105-125.

Kim J, Jeong JI, Kim KM, Choi I, Pratley RE, Lee YH. Improved glucose tolerance with restored expression of glucose transporter 4 in C57BL/6 mice after a long period of high-fat diet feeding. Animal Cells and Systems. 2014;18(3):197-203.

Li Z, Graham BH. Measurement of mitochondrial oxygen consumption using a Clark electrode. Mitochondrial Disorders: Biochemical and Molecular Analysis. 2012:63-72.

Lima FB, Machado UF, Bartol I, Seraphim PM, Sumida DH, Moraes SM, et al. Pinealectomy causes glucose intolerance and decreases adipose cell responsiveness to insulin in rats. American Journal of Physiology-Endocrinology and Metabolism. 1998; 275(6):E934-941.

Lin Y, Sun Z. Current views on type 2 diabetes. The Journal of endocrinology. 2010;204(1):1.

Lira VA, Benton CR, Yan Z, Bonen A. PGC-1α regulation by exercise training and its influences on muscle function and insulin sensitivity. American Journal of Physiology-

Endocrinology and Metabolism. 2010;299(2):E145-61.

Liu W, Son DO, Lau HK, Zhou Y, Prud'homme GJ, Jin T, et al. Combined oral administration of GABA and DPP-4 inhibitor prevents beta cell damage and promotes beta cell regeneration in mice. Frontiers in pharmacology. 2017;8:362.

Martínez-Reyes I, Chandel NS. Mitochondrial TCA cycle metabolites control physiology and disease. Nature communications. 2020;11(1):1-1.

Mohamed AS. Influence of Gamma Aminobutyric Acid on Some Biochemical Alterations in Irradiated and Streptozotocin Treated Rats. Ain Shams University. 2015.

Mulder H, Nagorny CL, Lyssenko V, Groop L. Melatonin receptors in pancreatic islets: good morning to a novel type 2 diabetes gene. Diabetologia. 2009;52(7):1240-9.

Nduhirabandi F, Du Toit EF, Blackhurst D, Marais D, Lochner A. Chronic melatonin consumption prevents obesity-related metabolic abnormalities and protects the heart against myocardial ischemia and reperfusion injury in a prediabetic model of diet-induced obesity. Journal of Pineal Research. 2011;50(2):171-82.

Nishida S, Sato R, Murai I, Nakagawa S. Effect of pinealectomy on plasma levels of insulin and leptin and on hepatic lipids in type 2 diabetic rats. Journal of pineal research. 2003; 35(4):251-6.

Nishida S, Segawa T, Murai I, Nakagawa S. Long-term melatonin administration reduces hyperinsulinemia and improves the altered fatty-acid compositions in type 2 diabetic rats via the restoration of Δ-5 desaturase activity. Journal of pineal research. 2002;32(1):26-33.

Oishi A, Cecon E, Jockers R. Melatonin receptor signaling: impact of receptor oligomerization on receptor function. International Review of Cell and Molecular Biology. 2018;338:59-77.

Owino S, Sánchez-Bretaño A, Tchio C, Cecon E, Karamitri A, Dam J, et al. Nocturnal activation of melatonin receptor type 1 signaling modulates diurnal insulin sensitivity via regulation of PI 3K activity. Journal of pineal research. 2018;64(3):e12462.

Pan M, Song YL, Xu JM, Gan HZ. Melatonin ameliorates nonalcoholic fatty liver induced by high-fat diet in rats. Journal of Pineal Research. 2006;41(1):79-84.

Patel R, Palit SP, Rathwa N, Ramachandran AV, Begum R. Genetic variants of tumor necrosis factor-α and its levels: A correlation with dyslipidemia and type 2 diabetes susceptibility. Clinical nutrition. 2019;38(3):1414-22.

Patel R, Parmar N, Rathwa N, Palit SP, Li Y, Garcia-Ocaña A, et al. A novel therapeutic combination of sitagliptin and melatonin regenerates pancreatic β-cells in mouse and human islets. Biochimica et Biophysica Acta (BBA)-Molecular Cell Research. 2022;1869 (8):119263.

Peschke E, Bähr I, Mühlbauer E. Melatonin and pancreatic islets: interrelationships between melatonin, insulin and glucagon. International journal of molecular sciences. 2013;14(4):6981-7015.

Peschke E, Frese T, Chankiewitz E, Peschke D, Preiss U, Schneyer U, et al. Diabetic Goto Kakizaki rats as well as type 2 diabetic patients show a decreased diurnal serum melatonin level and an increased pancreatic melatonin-receptor status. Journal of pineal research. 2006;40(2):135-43.

Peschke E, Mühlbauer E. New evidence for a role of melatonin in glucose regulation. Best practice & research Clinical endocrinology & metabolism. 2010;24(5):829-841.

Peschke E. Melatonin, endocrine pancreas and diabetes. Journal of Pineal Research. 2008;44(1):26-40.

Poon AM, Choy EH, Pang SF. Modulation of blood glucose by melatonin: a direct action on melatonin receptors in mouse hepatocytes. Neurosignals 2001;10(6):367-379.

Purwana I, Zheng J, Li X, Deurloo M, Son DO, Zhang Z, et al. GABA promotes human β-cell proliferation and modulates glucose homeostasis. Diabetes. 2014;63(12):4197-205.

Rathwa N, Parmar N, Palit SP, Patel R, Bhaskaran RS, Ramachandran AV, et al. Calorie restriction potentiates the therapeutic potential of GABA in managing type 2 diabetes in a mouse model. Life Sciences. 2022;295:120382.

Rezazadeh H, Sharifi MR, Sharifi M, Soltani N. Gamma-aminobutyric acid attenuates insulin resistance in type 2 diabetic patients and reduces the risk of insulin resistance in their offspring. Biomedicine & Pharmacotherapy. 2021;138:111440.

Ríos-Lugo MJ, Cano P, Jiménez-Ortega V, Fernández-Mateos MP, Scacchi PA, Cardinali DP, et al. Melatonin effect on plasma adiponectin, leptin, insulin, glucose, triglycerides and cholesterol in normal and high fat–fed rats. Journal of Pineal Research. 2010;49(4):342-348.

Rubio-Sastre P, Scheer FA, Gómez-Abellán P, Madrid JA, Garaulet M. Acute melatonin administration in humans impairs glucose tolerance in both the morning and evening. Sleep. 2014;37(10):1715-1719.

Scheer FA, Hilton MF, Mantzoros CS, Shea SA. Adverse metabolic and cardiovascular

consequences of circadian misalignment. Proceedings of the National Academy of Sciences. 2009;106(11):4453-8.

Shao W, Wang Z, Ip W, Chiang YT, Xiong X, Chai T, et al. GLP-1 (28–36) improves β-cell mass and glucose disposal in streptozotocin-induced diabetic mice and activates cAMP/PKA/β-catenin signaling in β-cells in vitro. American Journal of Physiology-Endocrinology and Metabolism. 2013;304(12):E1263-72.

Shieh JM, Wu HT, Cheng KC, Cheng JT. Melatonin ameliorates high fat diet-induced diabetes and stimulates glycogen synthesis via a PKCζ-Akt-GSK3β pathway in hepatic cells. Journal of pineal research. 2009;47(4):339-344.

Sohrabipour S, Sharifi MR, Talebi A, Sharifi M, Soltani N. GABA dramatically improves glucose tolerance in streptozotocin-induced diabetic rats fed with high-fat diet. European Journal of Pharmacology. 2018;826:75-84.

Stoscheck CM. [6] Quantitation of protein. InMethods in enzymology. 1990;182:50-68.
Stumpf I, Bazwinsky I, Peschke E. Modulation of the cGMP signaling pathway by melatonin in pancreatic β-cells. Journal of pineal research. 2009;46(2):140-7.

Taneera J, Jin Z, Jin Y, Muhammed SJ, Zhang E, Lang S, et al. γ-Aminobutyric acid (GABA) signalling in human pancreatic islets is altered in type 2 diabetes. Diabetologia. 2012;55(7):1985-94.

Tian J, Dang HN, Yong J, Chui WS, Dizon MP, Yaw CK, et al. Oral treatment with γ-aminobutyric acid improves glucose tolerance and insulin sensitivity by inhibiting inflammation in high fat diet-fed mice. PLoS one. 2011b;6(9):e25338.

Tuomi T, Nagorny CL, Singh P, Bennet H, Yu Q, Alenkvist I, et al. Increased melatonin signaling is a risk factor for type 2 diabetes. Cell metabolism. 2016;23(6):1067-77.

Wang S, Xiang YY, Zhu J, Yi F, Li J, Liu C, et al. Protective roles of hepatic GABA signaling in acute liver injury of rats. American Journal of Physiology-Gastrointestinal and Liver Physiology. 2017;312(3):G208-18.

Ye DW, Rong XL, Xu AM, Guo J. Liver-adipose tissue crosstalk: A key player in the pathogenesis of glucolipid metabolic disease. Chinese journal of integrative medicine. 2017;23(6):410-4.

Zalatan F, Krause JA, Blask DE. Inhibition of isoproterenol-induced lipolysis in rat inguinal adipocytes in vitro by physiological melatonin via a receptor-mediated mechanism. Endocrinology 2001;142(9):3783-3790.